Synthesis of Bimetallic (Ag-Au) Nanoparticles/Si Under Controlled Conditions Using A Laser-Assisted Wet KOH Etching Process

Aseel A.Chasb[1,a] **Ali A. Youssef** [1,b] **Alwan M. Alwan**[2,c]

[1] **Mustansiriyah University, College of Education, Physics Department**
[2] **University of Technology, Department of Applied Sciences**
[a)] aseel.ph.adel@gmail.com [b)] aliyousif73@gmail.com [c)] alkrzsm@yahoo.com.

Abstract:

Anisotropic KOH etchants are primarily used on this Si substrate to make pyramids on the surface of Si. Because the etching pathway is variable and random in nature, it is difficult to control over this process. Throughout this work, we used laser radiation to modify the topographical properties of Si substrates throughout the anisotropic during wet etching process with potassium hydroxide, as a highly effective, easy, and low-cost method of texturing Si substrates. The variations of illumination wavelength plays an important role in re surfaces texturing. Well-controlled formation bimetallic nano particles a uniform and dense aggregation of bimetallic nanoparticles was achieved; SERS active substrates with high efficiency were developed. Scanning electron microscopy (SEM) images, Atomic force microscopy (AFM), and X-Ray diffraction were used to evaluate the optical response of the textured surfaces.

Keywords: Si Texturing, wet KOH etching, bimetallic, SERS.

تخليق الجسيمات النانوية ثنائية المعدن (Ag-Au) في ظل ظروف معدلة باستخدام عملية حفر KOH الرطب بمساعدة الليزر

اسيل عادل جاسب[١] **أ.د.علي احمد يوسف**[١] **د. علوان محمد علوان**[٢]

[١] **الجامعة المستنصرية، كلية التربية، قسم الفيزياء**
[٢] **الجامعة التكنولوجية، قسم العلوم التطبيقية**

الملخص

يستخدم حفر هيدروكسيد البوتاسيوم متباين الخواص بشكل أساسي في ركيزة السليكون لصنع أهرامات على سطح ركيزة السليكون. نظرًا لأن مسار الحفر متغير وعشوائي بطبيعته، فمن الصعب التحكم في هذه العملية. خلال هذا العمل، استخدمنا إشعاع الليزر لتعديل الخصائص الطبوغرافية لركائز السليكون في جميع أنحاء ركيزة السليكون أثناء عملية الحفر الرطب مع هيدروكسيد البوتاسيوم، كطريقة فعالة للغاية وسهلة ومنخفضة التكلفة لتركيب ركائز السليكون. تلعب الاختلافات في الطول الموجي للإضاءة بالليزر دورًا مهمًا في تكوين الأسطح. تم التحكم جيدا بالجسيمات النانوية ثنائية المعدن وتم تحقيق تجميع موحد وكثيف للجسيمات النانوية ثنائية المعدن؛ تم تطوير ركائز نشطة SERS بكفاءة عالية. استخدام صور الفحص المجهري الإلكتروني (SEM) ومجهر القوة الذرية (AFM) وحيود الأشعة السينية لتقييم الاستجابة الضوئية لاسطح السليكون المخلقة.

الكلمات المفتاحية: حفر السليكون، حفر هيدروكسيد البوتاسيوم الرطب، ثنائي المعدن، استطارة رامان المعززة للسطح

1. Introduction:

Nanomaterials are nanoparticles with a diameter of less than 100 nm. The surface-to-mass or surface-to-volume ratios of these particles are extremely high. They may exhibit a range of physical, chemical, and biological properties that differ from those of their larger bulk counterparts[1].

Metallic nanoparticles are grouped as monometallic, bimetallic, trimetallic, and so on, based on their metallic composition[2]. Noble metallic NPs, such as gold nanoparticles, silver nanoparticles, or (Ag–Au) bimetallic NPs, have demonstrated a broad range of potential applications in antimicrobial agents, diagnostics, therapy, biosensing, drug delivery, and industrial catalysis. It is critical that nontoxic and safe NPs are prepared for use in these applications[3].

In the Si etching process wet chemical etching is a critical step in the process of fabricating a rough silicon surface. When etching monocrystalline silicon, KOH solutions are frequently used, as they can create Si textured layers with random pyramid or crater-like structures. However, due to the random nature of the etching pathway, this process is not well controlled [4]. Metal nanoparticles embedded in texturing Si have been thoroughly studied because of their specific optical properties. This work is directed to synthesis of bimetallic (Ag-Au) NPs and extensively investigated the laser's illumination effect on the KOH wet etching process in order to reconstruct the topographical characteristics of the Si surface to an optimal configuration for SERS sensing performance. The primary objective was to synthesize an active Si nanopillars layer for use in nanophotonics.

2. Experimental work

We used an n-type mirror like a Si wafer with a resistivity of (0.200 – 0.500) Ω.cm, 500µm thick, and (100) orientation. After cutting the substrate into 2 x 2 cm^2 parts and cleaning it with highly dilute 10% hydrofluoric acid, at a concentration of 3M KOH, the wet KOH texturizing process was carried out. The Si substrate during the wet etching process, it was irradiated. using a laser with a wavelength of approximately 650 nm and a fixed power density of approximately 150 mW/cm^3. The laser spot area was increased to encompass the entire Si surface area. All substrates were irradiated for approximately 2 minutes, and the effects of the laser wavelength on surface topography were investigated. Atomic force microscopy (AFM), contact mode type SPM-AA 3000 system was used to calculate the topographical characteristics (dimensions of nanopillars and textured surface shapes, roughness of the surface, and depth of nanopillars). The most critical point for modifying the properties of silver-gold nanoparticles is to modify the topographical characteristics of the rough Si surface to Si nanopillars layer that results. At constant immersion conditions, the plasmonic topographies of silver-gold nanoparticles vary according to the dimensions of the nanopillars, their density and shape, and their surface roughness. The bimetallic (Ag-Au) nanoparticles/Si nanopillars layers were synthesized by passivating the (silver-gold) ions on Si rough surfaces via a simple and quick dipping procedure. The rough Si surface and Si nanopillars were immersed in a $5x10^3$ M solution of (AgNPs and $HAuCl_4$) with a few drops of diluted 3 M HF for 3 minutes at room temperature. The optical properties of bimetallic NPs/Si texturing surface were investigated using scanning electron microscopy SEM (MIRA3 TESICAN) in conjunction with X-ray diffraction (XRD-6000, Shemadzuie).

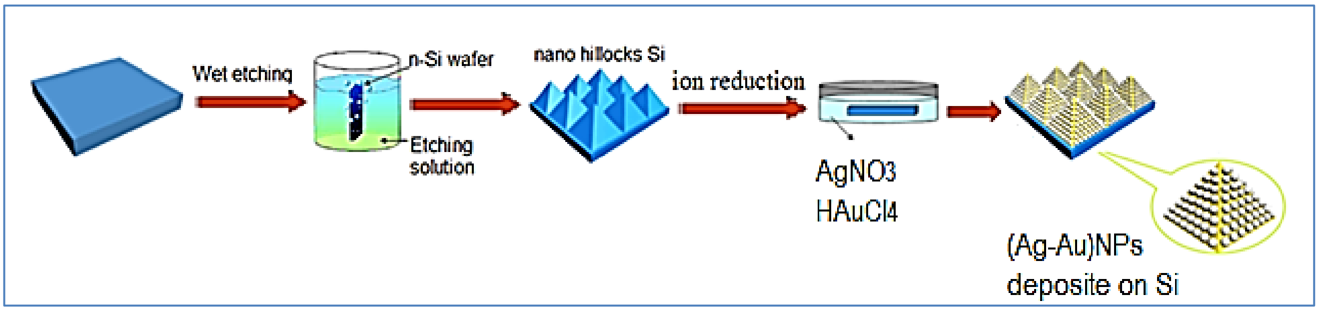

Figure1: present the schematic of the experimental part

3. Results and discussion:

3.1 Topographical Properties of bare Si Textured Substrates without laser assisted KOH etching process:

The topographical aspect of the bare textured silicon substrates as a function of KOH concentration solution (3) M are studied extensively. The topographical aspects of as- prepare textured Si substrate without laser illumination at 3M KOH concentration was explored as shown in figure 2. Without laser illumination, the 3D micro topographical image in figure 2(a) confirms that the Si rough structure's surface contains silicon nano Carter-like morphologies of varying sizes and shapes. These silicon cartridges are distributed randomly and have varying dimensions. The histogram of granularity of Si species as a function to KOH concentration is exposed in figure 2(b). The range of histogram was varied from (10 nm to 80 nm). The average height of nano carter were 37.74 nm. In addition, the surface roughness is specified for KOH concentration. It is clear that the average height of the nano carter and the surface roughness change as the KOH concentration changes. The average height of the carter and the roughness of surface reached to the highest value (37.74) nm, (4.76)nm respectively in 3M as show in table 1. The smallest nano carter dimension obtained in 3M KOH concentration is ranging from (10 to 80) nm with smallest an average nano size of about 70 nm.

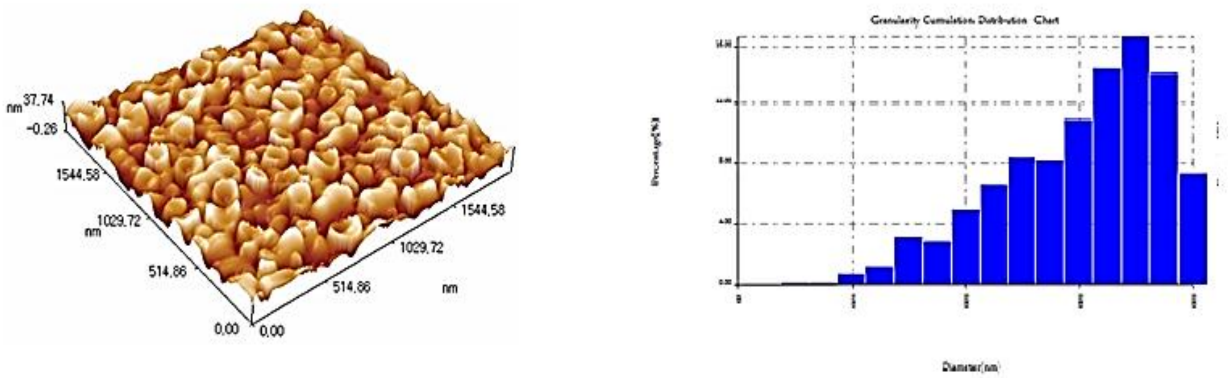

(a) (b)

Figure 2: a) 3D AFM images, (b) The histogram of granularity distribution of as-prepared surface textured silicon substrate without laser illumination at 3M KOH concentration.

3.2 Topographical Properties of bare Si Textured Substrates with laser assisted KOH etching process

The role of laser illumination wavelength on the characteristics of Si textured layer was studied. Laser wavelength about 650 nm at 150 mW/cm^2 laser illumination intensity to improve the surface topographies of silicon textured surface of substrate. The results of this condition is show in figure 3.

Figure 3(a) illustrates the 3D –AFM micro images of the textured silicon substrates prepared at 3M KOH concentration with using laser illumination 150 mW/cm^2 for 650 nm. While figure 3(b) illustrates the histogram of Si nanocrystallites as a function of laser illumination intensity.

For substrates with laser illumination of 650 nm, the three-dimensional microimage substrate's in figure 3(a) revealed a low of uniformity in nano pillars aligned within the Si surface. The histogram of granularity distribution figure 3(b) of Si Nano crystallites was varied with the laser illumination intensity variation. The range of Si dimension is about (20 nm to 90 nm). In addition, the average Si nano size is 55 nm for laser illumination intensity 150 mW/cm^2.

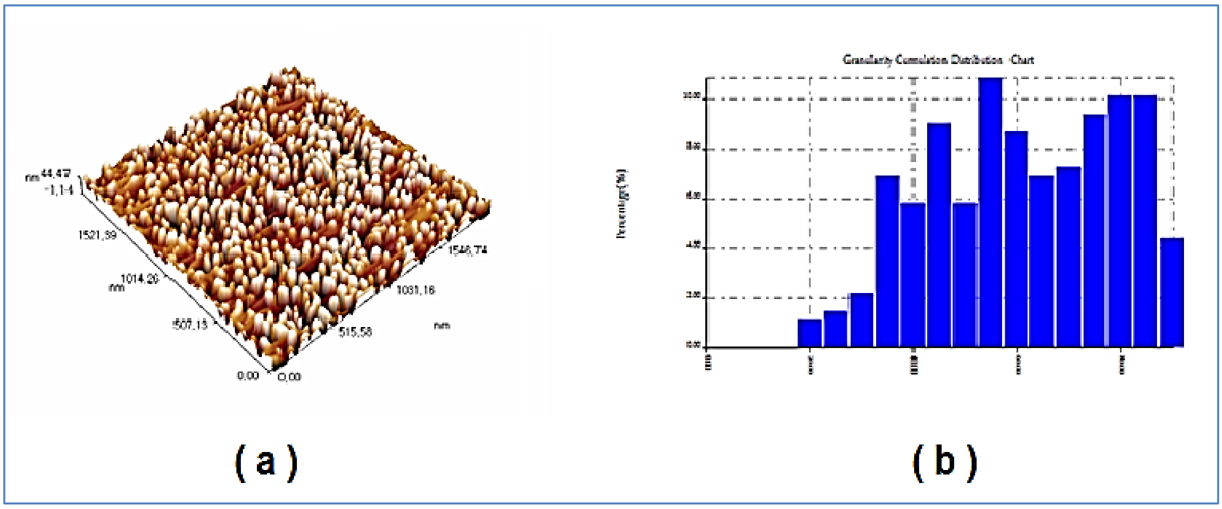

Figure 3: illustrate (a) 3D AFM images and (b) The histogram of granularity distribution of as-prepared surface textured silicon substrate under 650 nm laser wavelength at illumination intensity (150) mW/cm^2.

These modifications to silicon nanocrystallites' in-process wet etch surface topographies are strongly related to photon absorption and thus to the local increase in temperature within the area that has been irradiated. This increase in temperature enhances the process of dissolution of silicon, in both the x and y directions reducing the Carter's dimensions. This behavior increases the probability of changing Si morphologies from Carter to pillar. By increasing the laser wavelength, the probability of photons being absorbed deeply within the Si layer increases, resulting in an increase in the depth of the resulting nano crystallites (absorption in a z direction). According to the above-mentioned explanation, the use of etching with wet KOH and laser radiation can improve the results by increase the rate of Si engraving, thereby facilitating the Si solving process locally. To analyze the topographical characteristics of the textured silicon, the following criteria were used: The average height of hillocks, the surface's roughness, and the Si nano size. The first criterion of textured silicon is the Avg pillars height. It can be seen that the higher thickness that (44.47 nm) when use 650 nm laser wavelength, as shown in table 1.

Surface roughness is the second criterion for the textured Si. the surface roughness about (11.4) nm. Ultimately, this reflects the gradual growth of the pillars density, and the higher surface roughness of textured silicon about (11.4) nm when use 650 nm of laser wavelength as presented in table 1.

Table 1: The topographical properties of textured silicon substrates (a) without a laser and (b) with a laser at 650 nm.

	Average pillars height (nm)	Roughness (nm)	Si nanosize (nm)
(a)	37.74	4.76	70
(b)	44.47	11.4	55

3.3 AFM Analyses of the bimetallic (Ag-Au)NPs /Si textured structures

The study of the morphology of the (Ag-Au)NPs structure is very necessary because the SERS activity of the sensor depends on the (Ag-Au)NPs morphology [5]. In this section, the morphology of (Ag-Au)NPs deposited on the textured silicon samples prepared with laser illumination of KOH wet etching process with different morphology was studied at 3M KOH concentration and 2 min immersion time and laser wavelength 650 nm with power density 150 mW/cm^3.

Figure 4 show AFM images in 3D and granularity accumulation distribution chart of (Ag-Au)NPs deposited at 650 nm laser wavelength. AFM images provide relevant information regarding sample surfaces, from the obtained results of AFM and the related size distribution; it can be observed and deduced the following facts:

1- From AFM images, it is clear to us that the aggregation process becomes dominant process due to the progress of the nucleation.
2- The depth (Avg) of the resulted silicon nano hillocks was decreased due to the deposition of the metallic nanopartical.
3- The width of the resulting nanosize (Si+mettalic nanoparticals) was increased due the coating the silicon wall by metallic nanoparticals.
4- The minimum width is obtaind from the Ag/Au nano is about 60 nm.

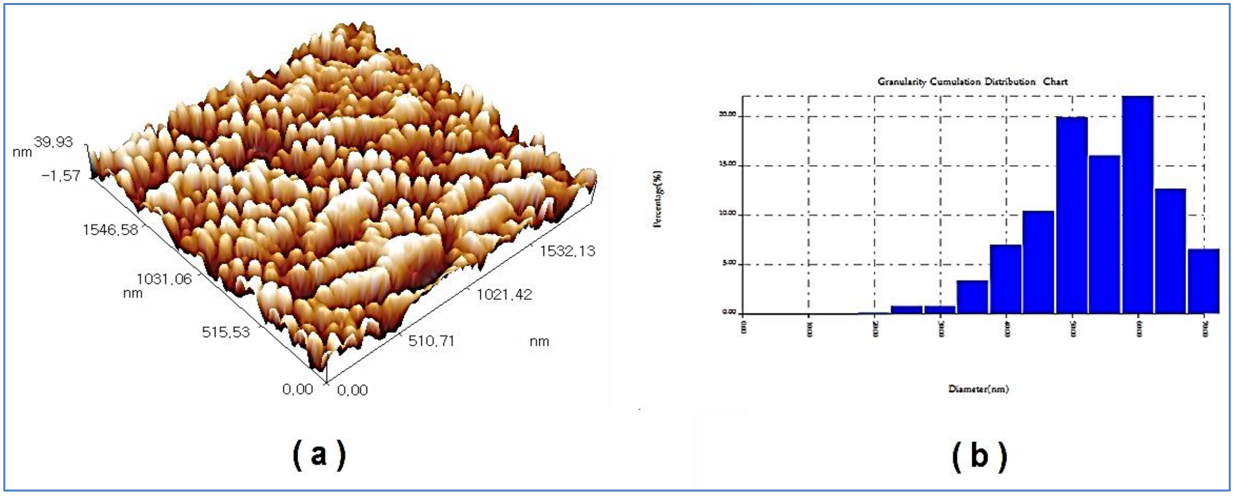

(a) (b)

Figure 4: (a) 3D AFM images and (b) histogram of granularity distribution of(Ag –Au)NPs deposited on textured silicon substrate at 3 M concentration with laser wavelength 650.

Table 2: Topographical features of (Ag-Au) NPs with 650 nm Laser wave length.

Material	**Average hillocks height (nm)**	**Roughness (nm)**	**Width of nano hilloks (nm)**
Ag-Au	39.93	12.6	60

3.5 SEM of the bimetallic (Ag-Au)NPs /Si textured structures

(Ag-Au) NPs associated into cluster have been observed over surface as shown in figure 5 which shows the surface morphology of the (Ag-Au)NPs deposited at on the textured silicon samples prepared with laser illumination of KOH wet etching process with different morphology was studied at 3M KOH concentration and 2 min immersion time with laser wavelength 650 nm and power density 150 mW/cm^3.

The surface morphology of bimetallic (Ag-Au)NPs deposited on Si textured surface as a function to laser illumination wavelength is illustrated in figure 5 in generally the forms of the resulted nanoparticles is looks like spherical nanoparticles with specific degree of aggregation. The dimensions of aggregated (Ag- Au) nanoparticles shows in figure 5 and therefore; Figure 5 (b,c), shows The sizes of the (Ag-Au)NPs are between 70 to 195 nm with peak of about 120 nm, while the hot spot's dimensions There are between 60 to 420 nm and the wavelength at which the peak intensity is achieved is 235 nm.

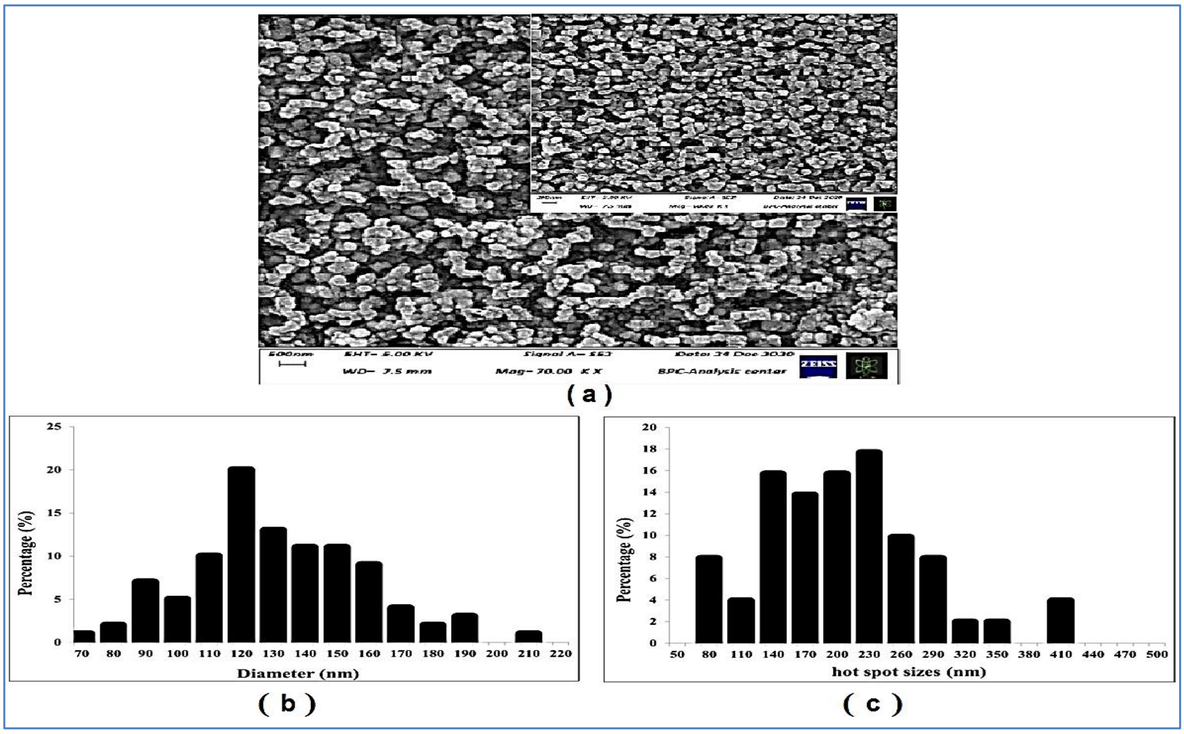

Figure 5: (a) illustrates the SEM images and magnified of (Ag-Au)NPs/Si nano crystallites, (b,c) shows the sizes of (Ag-Au)NPs and hot spot regions at 650 nm and illumination wavelength.

3.6 EDX analysis of the bimetallic (Ag-Au)NPs /Si textured structures

The confirmation of existence and the percentage of the forming bimetallic (Ag-Au)NPs on textured Si sample by ion reduction process was tested by measuring the EDX pattern as exposed in figure 6. The obtained result configures that at fixed laser illumination the rate of gold higher than that of silver due to the high tendency of Au ions to reach than that of Ag ions.

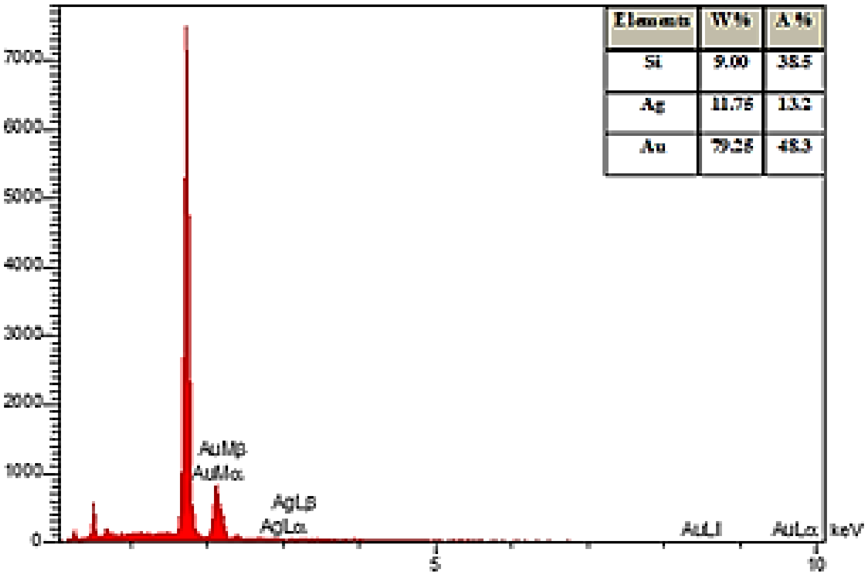

Element	W%	A%
Si	9.00	38.5
Ag	11.75	13.2
Au	79.25	48.3

Figure 6: illustrates the EDX analysis of bimetallic (Ag-Au)NPs as a function to illumination wavelength.

3.7 X-ray Diffraction pattern analysis of bimetallic (Ag-Au)NPs /Si textured structures

Figure 7 depicts the XRD pattern of (Ag-Au) nanoparticles/Si nanocrystallites synthesized by integrating Ag-Au nanoparticles on Si nanocrystallites substrates under laser illumination wavelength of 650 nm. This figure demonstrates that the Si-nanocrystallites are still in their crystalline phases along the (100) plane at a 2θ diffraction angle of approximately 32. 8°, 31.74°

whereas XRD analysis of Ag-Au nanoparticles reveals distinct Bragg's reflections with 2θ diffraction angle of approximately 38.2° and 44.4° for laser illumination wavelength 650nm which are assigned to the (111) and (200) crystalline planes of the (Ag-Au)NPs sensor respectively. They are compared to JCPDS codes 04– 0784 and 04–0783. This finding is consistent with those reported in the literature [6].

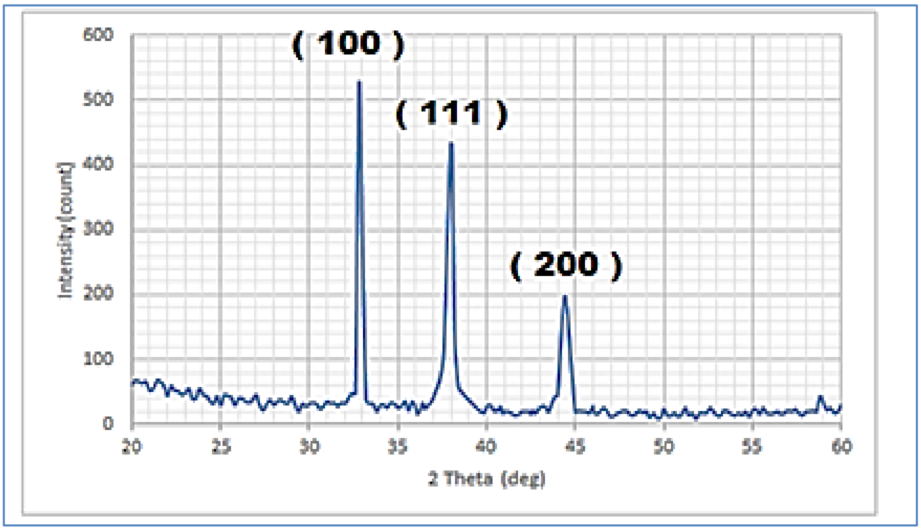

Figure 7: show the XRD of Si nanocrystallites/(Ag-Au) alloy laser illumination substrates at 650 nm laser wavelength.

When a laser source is used to illuminate the wet KOH etching process, the width at half maximum (FWHM) of the XRD peaks is boarded. This is due to the fact that the dimensions of the (Ag-Au) nanoparticles produced are directly related to them. The (FWHM) becomes wider as the size of the formed nanoparticles decreases. The laser illumination process used during wet KOH etching will alter the dimensions of Si nano crystallites and thus the synthesized nanoparticles. Using Scherer's equation[7], Based on XRD peak widening, the grain sizes of deposited (silver-gold) nanoparticles were calculated.

$$L= 0.9\lambda / B \cos\theta_B \qquad \dots (1)$$

Where (L) is the (Ag-Au) grain size in nanometers, (λ) is the applied radiation wavelength in nanometers, (B) is the radian value for the (FWHM), (θ_B) is the angle of diffraction in radians, and (0.9) is the value of the shape factor.

The specific surface area (S.S.A.) is very important limiting parameter for the characterization was calculated from equation:

$$\text{S. S. A} = 6000 / \text{grain size of NPs} * \rho \qquad \dots (2)$$

Where ρ denotes the bimetallic (Ag-Au) NPs nanoparticles density.
The structural parameters for (Ag-Au) NP are calculated from XRD results and the data are tabulated in the table 3.

Table 3: The structural parameters of (Ag-Au) NPs.

Materials	peaks	Grain size (nm)	S.S.A (nm)
(Ag-Au)NPs	**(100)**	13.33	----------
	(111)	12.73	44.87
	(200)	10.05	56.85

Conclusion

We report in this research. The modification of the wet KOH etching surface topography of synthesized Si nanocrystallites; this modification was accomplished through the illumination of the etching route with a laser. The surface's roughness, the shape, and the depth of Si nanocrystallites were determined by using a 650nm laser wavelength and a constant laser intensity. When the Si nanocrystallites were etched without illumination, there were large, irregular, Carter-like structures formed. The use of illumination by laser transforms the nanocrystallites that resulted are well-organized and uniformly distributed Si nanopillar-like structures with smaller dimensions. During the wet KOH etching process, The laser illumination increased Si dissolution within the layer of nano crystallites, resulting in more compact dimensions and greater depth. We developed easy, inexpensive, rapid, and well-controlled method for the formation of plasmonic bimetallic nanoparticles (dimensions and Specific surface area) on silicon nanocrystallites by using laser radiation with wet KOH. The obtained results add significant value to the field of bimetallic (silver-gold) nanoparticles.

Acknowledgments: The authors would like to thank Al-Mustansiriyah University (www.uomustansiriyah.edu.iq) Baghdad-Iraq and University of Technology, Baghdad-Iraq, for its support in the present work

References

[1] Y. Li and J. S. Church, "ScienceDirect Raman spectroscopy in the analysis of food and pharmaceutical nanomaterials," *J. Food Drug Anal.*, vol. 22, no. 1, pp. 29–48, 2014, doi: 10.1016/j.jfda.2014.01.003.

[2] Sumbal, A. Nadeem, S. Naz, J. S. Ali, A. Mannan, and M. Zia, "Synthesis, characterization and biological activities of monometallic and bimetallic nanoparticles using Mirabilis jalapa leaf extract," *Biotechnol. Reports*, vol. 22, p. e00338, 2019, doi: 10.1016/j.btre.2019.e00338.

[3] J. Li and Y. Weng, "Biosynthesis of Au , Ag and Au – Ag bimetallic nanoparticles using protein extracts of Deinococcus radiodurans and evaluation of their cytotoxicity," pp. 1411–1424, 2018.

[4] A. M. Alwan, A. A. Youssef, and A. A. Chasb, "Controllable synthesization of Au nanoparticles by laser enhanced wet KOH etching process," *J. Phys. Conf. Ser.*, vol. 1963, no. 1, p. 012009, 2021, doi: 10.1088/1742-6596/1963/1/012009.

[5] A. M. Alwan, A. A. Yousif, and L. A. Wali, "A Study on the Morphology of the Silver Nanoparticles Deposited on the n-Type Porous Silicon Prepared Under Different Illumination Types," *Plasmonics*, vol. 13, no. 4, pp. 1191–1199, 2018, doi: 10.1007/s11468-017-0620-3.

[6] A. M. Alwan, M. S. Mohammed, and R. M. Shehab, "Optimizing plasmonic characteristics of ag-aunps/nanohillocks si heterostructures for efficient sers performance," *Int. J. Nanoelectron. Mater.*, vol. 13, no. 2, pp. 323–340, 2020.

[7] A. A. Jabbar, A. M. Alwan, M. Q. Zayer, and A. J. Bohan, "Efficient single cell monitoring of pathogenic bacteria using bimetallic nanostructures embedded in gradient porous silicon," *Mater. Chem. Phys.*, vol. 241, no. August 2019, p. 122359, 2020, doi: 10.1016/j.matchemphys. 2019.122359.